Journal of Alloys and Compounds 566 (2013) 78–82

Contents lists available at SciVerse ScienceDirect

Journal of Alloys and Compounds

journal homepage: www.elsevier.com/locate/jalcom

Influence of coumarin as an additive on CuO nanostructures prepared by successive ionic layer adsorption and reaction (SILAR) method

F. Bayansal [a,*], B. Şahin [a], M. Yüksel [b], N. Biyikli [c], H.A. Çetinkara [a], H.S. Güder [a]

[a] Department of Physics, Faculty of Arts and Sciences, Mustafa Kemal University, Hatay, Turkey
[b] Department of Audiology, School of Health, Turgut Ozal University, Ankara, Turkey
[c] UNAM–National Nanotechnology Research Center, Bilkent University, Ankara, Turkey

ARTICLE INFO

Article history:
Received 20 February 2013
Received in revised form 7 March 2013
Accepted 8 March 2013
Available online 19 March 2013

Keywords:
CuO
SILAR
Band gap energy
Coumarin

ABSTRACT

The effect of coumarin doping during the growth of CuO nanostructures by SILAR method has been studied. It was found that coumarin considerably influences the growth process, manipulates the band-gap and modifies the crystallite size of the films. XRD experiments evidenced that with higher coumarin concentrations in the growth solution, the microstrain and dislocation density increased, while the crystallite size of the films decreased. SEM images revealed that the thicknesses of the plate-like nanostructures decreased with increasing coumarin concentration. By UV/vis spectrophotometer analysis it is found that the coumarin concentration affects both the optical band gap and the transmission rate: both the band gap and spectral transmittance values of the films decreased for higher coumarin content.

1. Introduction

Cupric oxide (CuO) is an important p-type transition-metal semiconductor with a relatively narrow band gap (~1.2 eV at room temperature) and has received considerable attention for various applications including gas sensors [1], biosensors [2], solar energy transformation [3], catalysis [4], batteries [5], and magnetic storage media [6]. Moreover, CuO is non-toxic, cost-effectively synthesized, and abundant in nature. Because of these properties, nanostructured CuO films have attracted significant research interest. A variety of growth techniques such as sputtering [7], electrodeposition [8], thermal oxidation/physical vapor deposition (PVD) [9], chemical vapor deposition (CVD) [10], sol–gel [11], chemical bath deposition (CBD) [12], and successive ionic layer adsorption and reaction (SILAR) [13] have been employed to synthesize and analyze CuO films. Among these techniques, SILAR is a promising technique because this technique is a relatively simple, safe, environmental friendly, suitable for mass production, low temperature compatible, and cost effective solution-based growth technique.

Various methods exist to manipulate the structural, optical, electrical and mechanical properties of solution-based grown thin films. One of these methods is using organic additives in the growth bath for solution-based synthesis. Additives in aqueous solutions are also known to control the surface morphology, preferred orientation, chemical composition, and the grain size [14]. A variety of additives such as coumarin, saccharin, citric acid, EDTA, malonic acid, and tartaric acid are the most widely used ones in electrodeposition processes for industrial coatings like nickel plating industry [15]. Among them, coumarin is known as an additive that not only refines the grains, but makes the grain size distribution more uniform as well [16]. It is well known that the properties of nano-crystalline/particular thin films depend on both the size and morphology of the crystals/particles. Many investigations are still carried out to improve the characteristics of CuO materials. However, to the best of our knowledge, the behavior of coumarin doping during the SILAR-based CuO film growth processes has not been studied yet. In this study, we investigate the influence of coumarin content on the morphology, crystalline structure, and optical properties of CuO nanostructured films obtained by SILAR method.

2. Experimental

The chemical reagents used in the experiments were analytical grade, purchased from Sigma–Aldrich Company and Merck KGaA and used without further purification. Before the film growth, the glass substrates were cleaned with dilute sulfuric acid solution (H_2SO_4:H_2O, 1:5, v/v), acetone, and double distilled water for 10 min. each in an ultrasonic bath. The growth bath was prepared as the following: 0.1 M copper chloride solution was prepared with copper(II) chloride dehydrate ($CuCl_2{\cdot}2H_2O$) and 100 ml double distilled water (18.2 MΩ cm^{-2}). The solution was stirred in a magnetic stirrer at room temperature for a few min. in order to get a transparent and well-dissolved solution. After stirring, pH value of the solution was adjusted to ~10.0 by adding aqueous ammonia and the solution was heated up to 90 °C at which the solution was kept during the entire growth phase. Pre-cleaned substrates were dipped into the growth bath vertically for 30 s. and then into hot water (90 °C) for another 30 s. This unit SILAR cycle was repeated for 10 times in order to get reasonably thick layers of nanostructured CuO film. When the growth process was finished the substrates were cooled down to room

* Corresponding author. Tel.: +90 326 2455845; fax: +90 326 2455867.
E-mail address: fbayy@hotmail.com (F. Bayansal).

0925-8388/$ - see front matter © 2013 Elsevier B.V. All rights reserved.
http://dx.doi.org/10.1016/j.jallcom.2013.03.018

temperature naturally and washed with water in an ultrasonic bath for 10 min. in order to remove the larger and loosely bonded CuO particles from the film surface. To investigate the effect of coumarin concentration, coumarin was added to the growth baths in certain concentrations as 1, 2, 4, 8, and 16 at.% respectively. The entire growth processes are the same as in the previously explained reference process where no coumarin was used. The only difference during the coumarin doping experiments is that after preparing the copper chloride solution, coumarin was added to the solution at the above-mentioned concentrations.

An FEI NOVA NANOSEM 430 scanning electron microscope (SEM) was used for morphological surface imaging. The crystal structure of the samples was examined by PANALYTICAL X'pert Pro MPD X-ray diffractometer (Cu Kα radiation, λ = 1.540056 Å). In order to measure the optical band gap values and investigate the spectral transmittance properties of the films, a THERMO 10S UV/vis spectrophotometer was used in the wavelength range of 190–1100 nm.

3. Results and discussion

3.1. Crystal structure and morphology

A FEI NOVA NANOSEM 430 scanning electron microscope (SEM) was used for morphological investigation of the synthesized CuO films. Fig. 1 shows typical SEM images of the CuO films obtained from the solutions containing 0, 1, 2, 4, 8, and 16 at.% coumarin, respectively. At the initial stage (without coumarin, Fig. 1a) there are plate-like CuO nanostructures which cover the whole surface homogenously. But with increased coumarin concentration, the nanostructures start to change their shapes, form some clusters on the surface and loose their homogeneity. The average thickness of the nanostructures in Fig. 1a is calculated as ~45 nm by using a pixels program. It was observed that the thickness of the plate-like nanostructures slowly decreased to ~34 nm (Fig. 1d and Table 1) and then they changed their shapes into flower-like nanostructures (Fig. 1e and f). These findings are in good agreement with our previous results on coumarin-doped ZnO nanostructures [16], in which small coumarin content (1 and 5 at.%) did not affect the microstructure but the higher concentrations affected the morphology excessively as seen in Fig. 1. Another significant observation is that the plate-like nanostructures are similar to the previously grown CuO nanostructures by our group utilizing the CBD method [17]. When compared to the CBD-grown nanostructures, SILAR-grown nanostructures did not form homogeneous

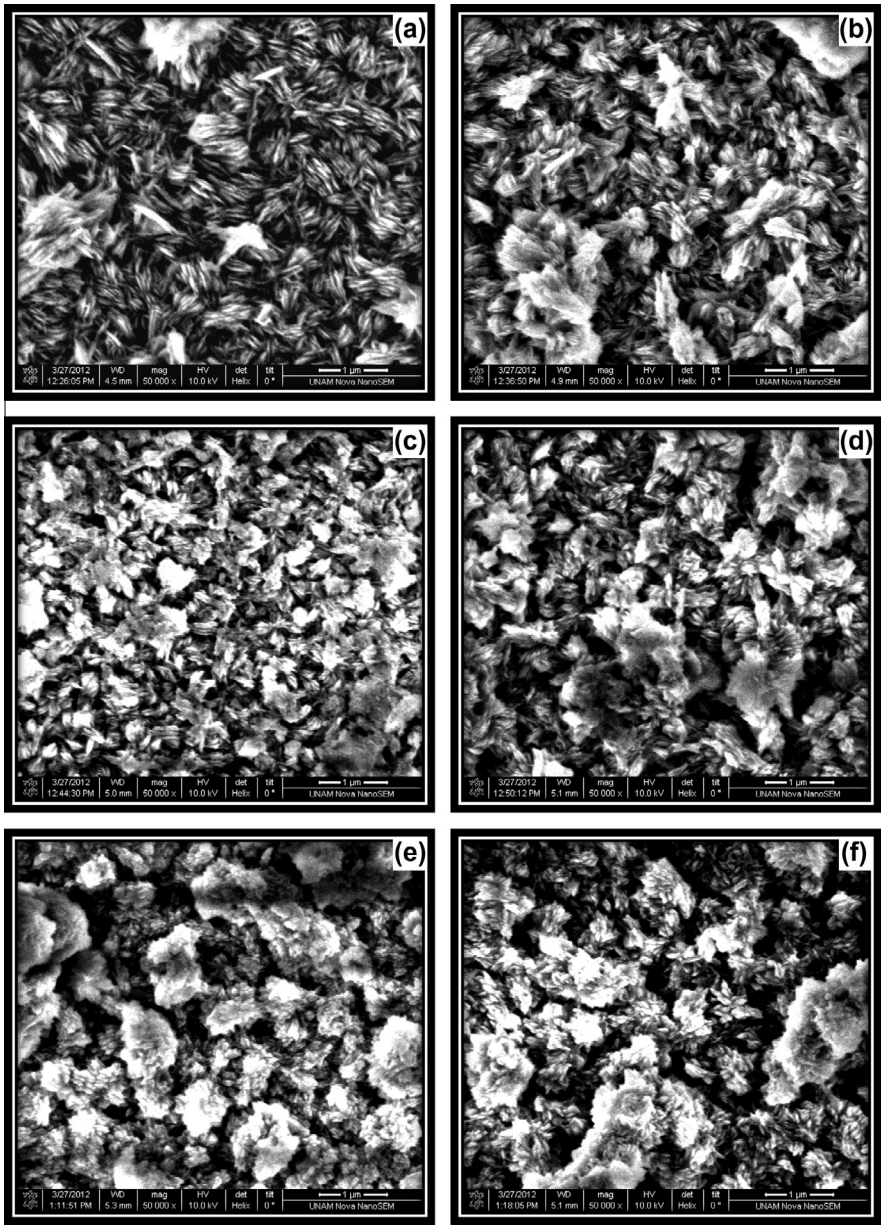

Fig. 1. SEM images of CuO films prepared in the solution having the coumarin concentrations of (a) 0%, (b) 1%, (c) 2%, (d) 4%, (e) 8% and (f) 16%.

Table 1
Plate thickness, average crystallite size, microstrain, dislocation density and band gap energy values of the CuO films as a function of coumarin concentration.

Coumarin concentration (%)	Plate thickness (nm)	Average crystallite size (D) (nm)	Microstrain (ε) $\times 10^{-3}$	Dislocation density (ρ) $\times 10^{12}$ (cm^{-2})	Band gap (eV)
0	45	18.6	1.95	33.5	1.50
1	39	16.9	2.15	41.0	1.44
2	38	14.7	2.47	54.1	1.43
4	34	15.9	2.28	46.1	1.39
8	–	15.5	2.33	48.1	1.34
16	–	15.0	2.41	51.6	1.32

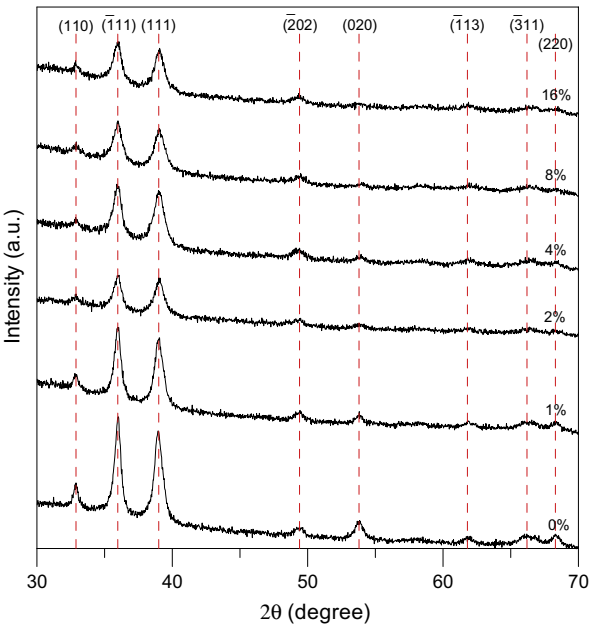

Fig. 2. XRD patterns of the CuO films.

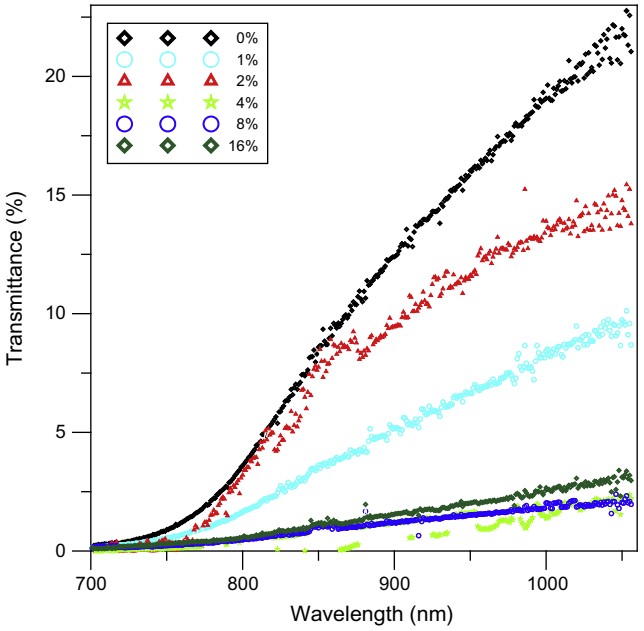

Fig. 3. Comparison of transmittance spectra of the CuO films as a function of coumarin concentration.

clusters, instead the CuO nanostructures spread over the entire substrate surface homogeneously.

To investigate the impact of coumarin concentration in the growth solution on the structural properties of the CuO nanostructures, X-ray diffraction (XRD) patterns of the samples were obtained at an operating voltage and current of 45 keV and 40 mA, respectively. The 2θ range of 30–70° was recorded at the rate of 0.02°. Fig. 2 shows typical XRD patterns of the synthesized CuO films. All diffraction peaks can be clearly indexed to the monoclinic CuO phase with lattice constants of $a = 4.6797$ Å, $b = 3.4314$ Å, $c = 5.1362$ Å and $\beta = 99.2620°$ (Reference code: 01-080-0076). From the figure it is clear that the Miller-indexed $(\bar{1}11)$ and (111) reflections are the strongest, which indicate that they are preferential crystal planes of the nanoplates. The other planes seen from the figure are (110), $(\bar{2}02)$, (020), $(\bar{1}13)$, $(\bar{3}11)$ and (220). From the patterns, one can deduce the following result: the coumarin concentration in the growth solution has a diminishing effect on the peak intensities. The preferential plane intensities decreased with increasing coumarin content but did not disappear completely. On the other hand, most of the week peaks disappeared with increasing coumarin content which means that the crystal structure deteriorates at high coumarin concentrations.

The average crystallite sizes (D) of the CuO nanostructures was calculated from the peak full width at the half maximum (FWHM) of a peak (β), using the Debye–Scherrer's equation [16]:

$$D = \frac{0.94\lambda}{\beta \cos\theta} \tag{1}$$

where λ is the wavelength of X-ray radiation, θ is the Bragg's angle of the peaks and β is the angular width of peaks at FWHM. Each X-ray diffraction peak obtained in a diffractometer is broadened due to instrumental and physical factors. The microstrain (ε) and dislocation density (ρ) for the CuO films were calculated using the following equations [18]:

$$\varepsilon = \frac{\beta \cos\theta}{4} \tag{2}$$

and

$$\rho = \frac{15\varepsilon}{aD} \tag{3}$$

where a is the lattice constant. The calculated average crystallite sizes (D) of the CuO nanostructures are given in Table 1. As seen from the table, crystallite sizes of the films decrease with increasing coumarin content. This result can also be supported by SEM measurements. As expected, both the microstrain and dislocation density values of the films increased (due to the decrease in the grain size) with increasing coumarin concentration. From a detailed investigation of XRD patterns, a shift in peak positions was determined towards higher 2θ values with increasing coumarin concentration. This shift indicates the presence of an increasing lattice strain in the film structure [19]. In Bragg's formula ($2d \sin\theta = n\lambda$), a decrease of the interplanar spacing, as a consequence of lattice strain induced in the structure during preparation procedure by

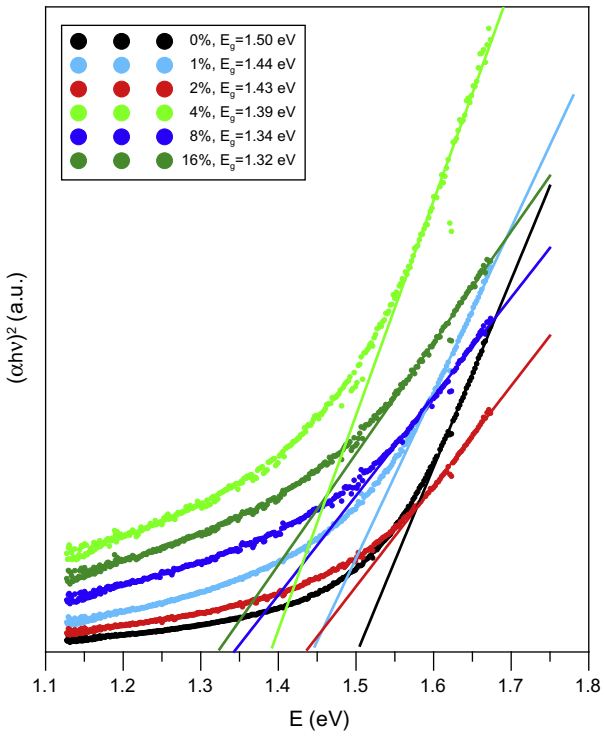

Fig. 4. Comparison of $(\alpha h\upsilon)^2$ versus $h\upsilon$ plots of the CuO films as a function of coumarin concentration.

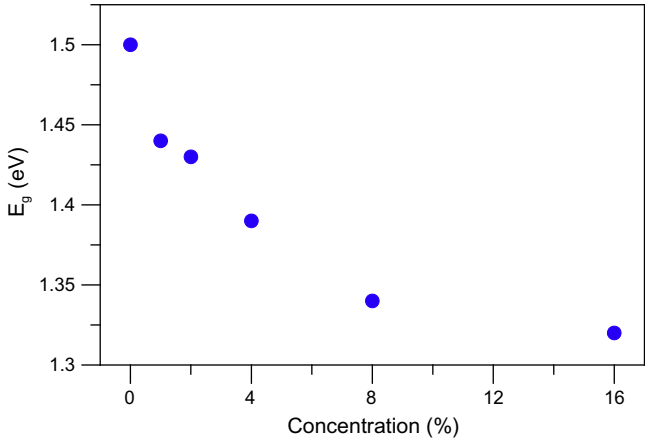

Fig. 5. Band gap values of the CuO films as a function of coumarin concentration.

various factors such as impurities, lattice defects, vacancies or deformation faults, implies a shift to a higher Bragg angle [20].

3.2. Optical investigations

In order to measure the band gap energies and investigate the transmittance properties of the films, a THERMO 10S UV–vis. spectrophotometer was used in the wavelength range of 190–1100 nm. The transmittance spectra as a function of coumarin concentration recorded in the wavelength range of 700–1050 nm are shown in Fig. 3. The CuO film without coumarin content has the highest transmittance (~23%) at longer wavelengths. The transmittance decreased rapidly with increasing coumarin concentration. The films having the plate-like nanostructures have higher transmittance than the films having the flower-like nanostructures. As the coumarin concentration reaches 4 at.% and beyond, the transmittance decreases under 2%. The optical absorption in the UV–vis. region is dominated by the optical band gap (E_g) of a semiconductor that is related to the optical absorption coefficient (α) and the incident photon energy ($h\upsilon$) by the following relation:

$$(\alpha h\upsilon) = C(h\upsilon - E_g)^m \quad (4)$$

where C is an energy independent constant and m is an index which depends on the kind of optical transition that prevails [21,22]. Specifically, n is 1/2, 3/2, 2 and 3 when the transition is direct-allowed, direct-forbidden, indirect-allowed, and indirect-forbidden respectively. CuO film is known to be a direct-allowed semiconductor, and hence a graph was plotted (Fig. 4) with $(\alpha h\upsilon)^2$ (where $m = 1/2$) versus photon energy ($h\upsilon$) as a function of coumarin concentration. Using this graph, the band gap values can be determined by extrapolating the straight line portion. The E_g values were found to be 1.50, 1.44, 1.43, 1.39, 1.34 and 1.32 eV for the films which were grown in the baths having 0, 1, 2, 4, 8 and 16 at.% of coumarin concentrations respectively. The band gap values versus coumarin concentration in the growth solution are plotted in Fig. 5. It was seen that the E_g values of the films decreased with increasing coumarin content which means that the coumarin as an additive can be used as a regulator of the band gap of a semiconductor.

4. Conclusion

The effect of coumarin as an additive in the growth solution in a SILAR process of CuO films was investigated. We conclude that the morphology, crystal structure, band gap and transmittance of the films were affected considerably by coumarin concentration. With increasing coumarin concentration in the growth solution, the microstrain and dislocation density values increased, while the band gap energy values, transmittance and crystallite sizes of the nanostructures decreased. Moreover, the nanostructured films changed their morphology from plate-like nanostructures to flower-like nanostructures. The most important conclusion of this study is that we have shown the effect of coumarin as a regulator on the band gap energy values. This influence can potentially be used in electronics, opto-electronics, and optical applications where band gap engineering becomes an important degree of freedom to design optimal device structures for various technologies.

Acknowledgements

This work is financially supported by the Scientific Research Commission of Mustafa Kemal University (Project No: 1001 M 0115). N.B. acknowledges Marie Curie International Reintegration Grant (IRG) for funding NEMSmart (PIRG05-GA-2009-249196) project.

References

[1] H.T. Hsueh, T.J. Hsueh, S.J. Chang, F.Y. Hung, T.Y. Tsai, W.Y. Weng, C.L. Hsu, B.T. Dai, CuO nanowire-based humidity sensors prepared on glass substrate, Sens. Actuators B 156 (2011) 906–911.
[2] X. Wang, C. Hu, H. Liu, G. Du, X. He, Y. Xi, Synthesis of CuO nanostructures and their application for nonenzymatic glucose sensing, Sens. Actuators B 144 (2010) 220–225.
[3] H. Chang, M.J. Kao, K.C. Cho, S.L. Chen, K.H. Chu, C.C. Chen, Integration of CuO thin films and dye-sensitized solar cells for thermoelectric generators, Curr. Appl. Phys. 11 (2011) 19–22.
[4] F. Teng, W. Yao, Y. Zheng, Y. Ma, Y. Teng, T. Xu, S. Liang, Y. Zhu, Synthesis of flower-like CuO nanostructures as a sensitive sensor for catalysis, Sens. Actuators B 134 (2008) 761–768.
[5] C. Li, W. Wei, S. Fang, H. Wang, Y. Zhang, Y. Gui, R. Chen, A novel CuO-nanotube/SnO_2 composite as the anode material for lithium ion batteries, J. Power Sources 195 (2010) 2939–2944.
[6] W. Gao, S. Yang, S. Yang, L. Lv, Y. Du, Synthesis and magnetic properties of Mn doped CuO nanowires, Phys. Lett. A 375 (2010) 180–182.
[7] J.K. Feng, H. Xia, M.O. Lai, L. Lu, Electrochemical performance of CuO nanocrystal film fabricated by room temperature sputtering, Mater. Res. Bull. 46 (2011) 424–427.

[8] N. Mukherjee, B. Show, S.K. Maji, U. Madhu, S.K. Bhar, B.C. Mitra, G.G. Khan, A. Mondal, CuO nano-whiskers: electrodeposition Raman analysis, photoluminescence study and photocatalytic activity, , Mater. Lett. 65 (2011) 3248–3250.
[9] L.D.L.S. Valladares, D.H. Salinas, A.B. Dominguez, D.A. Najarro, S.I. Khondaker, T. Mitrelias, C.H.W. Barnes, J.A. Aguiar, Y. Majima, Crystallization and electrical resistivity of Cu_2O and CuO obtained by thermal oxidation of Cu thin films on SiO_2/Si substrates, Thin Solid Films 520 (2012) 6368–6374.
[10] F.P. Albores, W.A. Flores, P.A. Madrid, E.R. Valdovinos, M.V. Zapata, F.P. Delgado, M.M. Yoshida, Growth and microstructural study of CuO covered ZnO nanorods, J. Cryst. Growth 351 (2012) 77–82.
[11] S. Das, S. Majumdar, S. Giri, Room temperature weak ferromagnetism and magnetoconductance in functional CuO film, Appl. Surf. Sci. 257 (2011) 10775–10779.
[12] F. Bayansal, H.A. Çetinkara, S. Kahraman, H.M. Çakmak, H.S. Güder, Nanostructured CuO films prepared by simple solution methods: plate-like, needle-like and network-like architectures, Ceram. Int. 38 (2012) 1859–1866.
[13] A.A. Taysioglu, A. Peksoz, Y. Kaya, N. Derebasi, G. Irez, G. Kaynak, GMI effect in CuO coated Co-based amorphous ribbons, J. Alloys. Comp. 487 (2009) 38–41.
[14] M.H. Gharahcheshmeh, M.H. Sohi, Study of the corrosion behavior of zinc and Zn–Co alloy electrodeposits obtained from alkaline bath using direct current, Mater. Chem. Phys. 117 (2009) 414–421.
[15] L.P. Bicelli, B. Bozzini, C. Mele, L. D'Urzo, A review of nanostructural aspects of metal electrodeposition, Int. J. Electrochem. Sci. 3 (2008) 356–408.
[16] H.M. Çakmak, S. Kahraman, F. Bayansal, S. Çetinkaya, A novel study on ZnO nanostructures: coumarin effect, Philos. Mag. Lett. 92 (2012) 288–294.
[17] F. Bayansal, S. Kahraman, G. Çankaya, H.A. Çetinkara, H.S. Güder, H.M. Çakmak, Growth of homogenous CuO nano-structured thin films by a simple solution method, J. Alloys. Comp. 509 (2011) 2094–2098.
[18] S. Kahraman, H.A. Çetinkara, F. Bayansal, H.M. Çakmak, H.S. Güder, Characterisation of ZnO nanorod arrays grown by a low temperature hydrothermal method, Philos. Mag. 92 (2012) 2150–2163.
[19] G.G. Rusu, A.P. Rambu, V.E. Buta, M. Dobromir, D. Luca, M. Rusu, Structural and optical characterization of Al-doped ZnO films prepared by thermal oxidation of evaporated Zn/Al multilayered films, Mater. Chem. Phys. 123 (2010) 314–321.
[20] A.A. Dakhel, F.Z. Henari, Optical characterization of thermally evaporated thin CdO films, Cryst. Res. Technol. 38 (2003) 979–985.
[21] H.M. Çakmak, H.A. Çetinkara, S. Kahraman, F. Bayansal, M. Tepe, H.S. Güder, M.A. Çipiloğlu, Effects of thermal oxidation temperature on vacuum evaporated tin dioxide film, Superlattices Microstruct. 51 (2012) 421–429.
[22] J.I. Pankove, Optical Processes in Semiconductors, Prentice-Hall, NJ, 1971. p. 34.